Prospects of detecting m_e/m_p variance using vibrational transition frequencies of $^2\Sigma$-state molecules

Masatoshi Kajita*

National Institute of Information and Communications Technology, Nukui-Kitamachi, Koganei, Japan

(Received 15 October 2007; revised manuscript received 10 November 2007; published 24 January 2008)

This paper discusses the possibility of measuring the variance in the electron-to-proton mass ratio β using the $|X\,^2\Sigma,\ n_v=0,\ N=0,\ J=1/2,\ F=1,\ M_F=1\rangle \rightarrow |X\,^2\Sigma,\ n_v=1$ or 2, $N=0,\ J=1/2,\ F=1, M_F=1\rangle$ transition frequencies of magnetically trapped cold ^{24}MgH or ^{40}CaH molecules. The uncertainty in this transition frequency can potentially be lower than 10^{-15}, which makes it possible to measure the variance in β. The ^{24}MgH transition is more advantageous for measurement than the ^{40}CaH transition, because of the lower collision-loss rate, light shift, and collision shift.

DOI: 10.1103/PhysRevA.77.012511 PACS number(s): 33.20.−t, 06.30.Ft, 34.10.+x

I. INTRODUCTION

Possible variations in nature's fundamental constants are currently a very popular topic in research. Theories unifying gravity and other interactions suggest the possibility of spatial and temporal variations in the physical constants of the universe [1]. Webb *et al.* found variance in the fine structure constant, α, in quasars (the absorption red shift was between 0.5 and 3.5) as $\Delta\alpha/\alpha=(-0.72\pm0.18)\times10^{-5}$ [2]. Reinhold *et al.* found variance in the electron-to-proton mass ratio, $\beta(=m_e/m_p)$, in quasars (the absorption red shift was between 2.59 and 3.02) as $\Delta\beta/\beta=(2\pm0.59)\times10^{-5}$ [3]. By comparing highly accurate atomic (or molecular) clocks, variations in the fundamental constants can be detected in a laboratory.

The accuracy of atomic clocks has been improved by using ultracold atoms or ions. The frequency uncertainty of the Cs atomic fountain frequency standard is presently less than 10^{-15} [4]. The frequency uncertainties of *S-D* transitions in $^{199}Hg^+$ [5], $^{171}Yb^+$ [6], and $^{88}Sr^+$ [7] ions are presently 9.1×10^{-16}, 3.8×10^{-15}, and 3.4×10^{-15}, respectively. The ^{87}Sr $^1S_0-{}^3P_0$ transition frequency was measured by Boyd *et al.* within an accuracy of 9×10^{-16} [8]. The value of $(d\alpha/dt)/\alpha$ is presently $(-0.3\pm2)\times10^{-15}$ years [9], and its uncertainty is expected to be further reduced as the accuracies of atomic clocks are improved. Hudson *et al.* measured the microwave transition frequencies of cold OH molecules within an accuracy of 3×10^{-9}, aiming at the measurement of $(d\alpha/dt)/\alpha$ through comparisons with measurements from OH megamasers in interstellar space [10].

Calmet and Fritzsch have shown $(d\beta/dt)/\beta=R_c(d\alpha/dt)/\alpha$, where R_c is a value between −20 and −40 [11]. Variances in α and β provide very important information on grand unification theory (GUT), because the actual value of R_c depends on the details of this theory. However, variations in β cannot be measured using atomic transitions, because the atomic energy states are only determined by the motion of electrons (not nuclei). Variance in β can be observed by comparing molecular-vibrational or rotational-transition frequencies. Schiller and Korobov showed the theoretical dependence of the vibrational-rotational-transition frequencies of H_2^+ ions on β [12]. Assuming that $(d\beta/dt)$ is constant for 10^{10} years, $(d\beta/dt)/\beta$ can be estimated to be on the order of 2×10^{-15} years^{-1}. Therefore, molecular-vibrational ($\propto\beta^{1/2}$) or rotational-transition ($\propto\beta$) frequencies with uncertainties lower than 10^{-15} are useful for measuring the variance in β. However, molecular-transition frequencies have mostly been measured at room temperature, as it has been difficult to obtain cold molecules. The uncertainty of molecular transitions could not be lower than 10^{-11} [13] because of the short interaction time between molecules and probing electromagnetic radiation and the Doppler effect. Roth *et al.* observed the rovibrational spectrum of HD^+ ions after sympathetic cooling with laser-cooled Be^+ ions [14]. The influence of the electric field on the transition frequency can be significant with this method, unless all HD^+ ions are positioned at zero-electric field positions. Van Veldhoven *et al.* improved the resolution of the ND_3 inversion spectrum using a decelerated molecular beam [15]. The interaction time between molecules and the probing microwave cannot be longer than 10 ms (the linewidth cannot be narrower than 16 Hz) with this method.

Our last paper, Ref. [16], proposed the use of the ^{14}NH $|X\,^3\Sigma, n_v=0, N=0, J=1, F_1=3/2, F=5/2, M_F=5/2\rangle \rightarrow |X\,^3\Sigma, n_v=1, N=0, J=1, F_1=3/2, F=5/2, M_F=5/2\rangle$ transition frequency to measure the variance in β, where n_v is the vibrational quantum number, N is the quantum number of molecular rotation, and J is $N+S$ (S is electron spin). Here, F_1 is $J+I$(H) [I(H): H nuclear spin], F is F_1+I(N) [I(N): N nuclear spin], and M_D is the component of $D(=F,N,S,I)$ parallel to the magnetic field. The NH molecules are trapped by the magnetic field after cooling them with cold buffer gas [17]. The interaction time between molecules and the probe laser light can be longer than 1 s. Assuming pure rotational states, M_S and $M_{I(\mathrm{N,H})}$ are deterministic values in the $|N=0, M_F=S+I(\mathrm{N})+I(\mathrm{H})\rangle$ state. The Zeeman frequency shift is smaller than 10^{-15} for the $|X\,^3\Sigma, n_v=0, N=0, J=1, F_1=3/2, F=5/2, M_F=5/2\rangle \rightarrow |X\,^3\Sigma, n_v=1, N=0, J=1, F_1=3/2, F=5/2, M_F=5/2\rangle$ transition. This treatment (also as quoted in Ref. [16]) poses some problems, because spin-spin interaction [18] induces the mix between $|N=0, M_S=1\rangle$ and $|N=2, M_S=1, 0, -1\rangle$ states, that depends on the rotational constant in each vibrational state. Therefore,

*kajita@nict.go.jp

the dependence of the Zeeman coefficient on the vibrational state is actually much more significant than estimated in Ref. [16]. The Zeeman frequency shift of the $|X\,^3\Sigma, n_v=0, N=0, J=1, F_1=3/2, F=5/2, M_F=5/2\rangle \rightarrow |X\,^3\Sigma, n_v=1, N=0, J=1, F_1=3/2, F=5/2, M_F=5/2\rangle$ transition is on the order −18 Hz/G (see Appendix A). The complicated hyperfine structure is also a problem, because only molecules in one of eighteen hyperfine substates are used for measurement.

This paper discusses the potential accuracies of the $|X\,^2\Sigma, n_v=0, N=0, J=1/2, F=1, M_F=1\rangle \rightarrow |X\,^2\Sigma, n_v=1$ or $2, N=0, J=1/2, F=1, M_F=1\rangle$ transition frequencies of ^{24}MgH or ^{40}CaH molecules. The Doyle group at Harvard succeeded in the magnetic trapping of CaH molecules after precooling using buffer gas [19]. There is no spin-spin interaction by molecules in the $^2\Sigma$ state [18] and the Zeeman shift in the transition frequency is much lower than the one for NH transition. Also note that ^{24}Mg and ^{40}Ca atoms have no nuclear spin and there are only four hyperfine substates for ^{24}MgH and ^{40}CaH molecules. ^{24}MgH and ^{40}CaH molecules are more advantageous for obtaining a high S/N ratio for the transition spectrum than ^{14}NH molecules, because a higher fraction of molecules is used for measurement.

Section II discusses the elastic and inelastic collisions between trapped molecules, which indicate the possibility of evaporative cooling. Section III presents estimates of frequency shifts induced by electric-magnetic-field or Doppler effects. Section IV presents the experimental procedure to measure the transition frequency.

II. COLLISION BETWEEN TRAPPED MOLECULES

Evaporative cooling is a useful method of reducing the temperature of trapped molecules. Fried *et al.* observed Bose-Einstein condensation with H atoms [20] by only using evaporative cooling. Evaporative cooling is achieved by irradiating a microwave (frequency f_{ev}) to the magnetically trapped molecules (the magnetic field is zero at the trap center). Then, molecules with trapping vibrational energies E_{trap} (kinetic energy + Zeeman potential energy) higher than $E_{\mathrm{max}}=h\mu_B f_{\mathrm{ev}}/2$ are transformed to the $M_S=-1/2$ state and repelled from the trap area. The energy distribution is not thermal equilibrium at this moment. Assuming $E_{\mathrm{max}} \ll k_B T_{\mathrm{in}}$ (T_{in} is the initial molecular temperature), the mean value of Zeeman potential energy at this moment is (selection of low energy molecules):

$$(E_{\mathrm{trap}})_{\mathrm{av}}^{\mathrm{noneq}} = k_B T_{\mathrm{in}} - \frac{h\mu_B f_{\mathrm{ev}}}{2} \frac{1}{\exp\left(\frac{h\mu_B f_{\mathrm{ev}}}{2k_B T_{\mathrm{in}}}\right) - 1} \approx \frac{E_{\mathrm{max}}}{2}. \tag{1}$$

When the magnetic field distribution is given by $B \propto R^{n_B}$ (R is the molecular displacement from the trap center), the mean values of kinetic energy K and Zeeman potential energy E_Z are given by the virial law as

$$(K)_{\mathrm{av}} \approx \frac{n_B}{n_B+2} \frac{E_{\mathrm{max}}}{2},$$

$$(E_Z)_{\mathrm{av}} \approx \frac{E_{\mathrm{max}}}{n_B+2}. \tag{2}$$

The selection of low energy molecule is possible also by reducing the trapping potential depth, as Weinstein *et al.* performed with Cr atoms [21]. There is also adiabatic cooling effect with this method.

The energy distribution is transformed to the thermal equilibrium state with temperature T_{eq}. Molecules, whose Zeeman potential energy increased up to E_{max}, are extracted with this procedure and $(E_{\mathrm{trap}})_{\mathrm{av}}$ of trapped molecules is further reduced (evaporative cooling). T_{eq} is actually on the order of $E_{\mathrm{max}}/10k_B$ [22]. This thermalization time τ_{th} is much longer than $1/\Gamma_{\mathrm{ec}}$, where Γ_{ec} is the elastic collision rate. The trap-loss rate Γ_{loss} should be sufficiently small so that $\Gamma_{\mathrm{loss}}/\Gamma_{\mathrm{ec}} \ll \tau_{\mathrm{th}}\Gamma_{\mathrm{loss}} < 1$ is satisfied. Monroe *et al.* found that evaporative cooling is only effective when $\Gamma_{\mathrm{loss}}/\Gamma_{\mathrm{ec}}$ is smaller than 1/150 [23]. Giving E_{max} initially higher than $k_B T_{\mathrm{in}}$ and reducing it slowly down to the final value E_{max}^f (taking longer time than τ_{th}), much more molecules remain in the trapping region than when $E_{\mathrm{max}}=E_{\mathrm{max}}^f$ from the beginning [22].

From molecules in $|S=1/2, M_S=\pm 1/2\rangle$ states, only molecules in the $M_S=1/2$ state are trapped in a field minimum of a dc magnetic field. The $M_S=1/2 \rightarrow -1/2$ transition (induced by the collision with other trapped molecules or background gas, pumping by blackbody radiation [24], or Majorana transition [25]) causes the trap loss. When the density of the trapped molecules is sufficiently high, $\Gamma_{\mathrm{loss}}/\Gamma_{\mathrm{ec}}$ converges to the ratio of the inelastic collision cross section to the elastic collision cross section. We estimated the elastic and inelastic collision cross sections between trapped ^{24}MgH and between ^{40}CaH molecules in the $^2\Sigma$ $N=0$ state. The values for permanent dipole moment and rotational constants in the vibrational ground state are listed in Table I [26–30].

Elastic collision is mainly induced by electric dipole-induced dipole interaction, and the elastic-collision cross section σ_e is obtained from the distortion of the incident wave function [31]. The M_S-changing collisional transition is caused by magnetic dipole-dipole or spin-rotation interactions. Spin-rotation interaction does not exist for the pure $N=0$ state. The mixture of different rotational states is only caused by electric field E, because spin-spin interaction does not exist for molecules in the $^2\Sigma$ state. The mixture of rotational states is estimated by $c_{\mathrm{mix}}=\mu_{n_v}E/hB_{n_v}$, where μ_{n_v} and B_{n_v} are the permanent dipole moment and the rotational constant in the n_vth vibrational state, respectively. Using the values of μ_0 and B_0 listed in Table I, c_{mix} is estimated to be smaller than 10^{-4} when $E<10$ V/cm; thus the M_S-changing inelastic collision is mainly caused by the magnetic dipole-dipole interaction. The inelastic-collision cross sections σ_i were obtained using Born approximation taking the distortion in the wave function caused by electric dipole-induced dipole interaction into account (distorted wave Born approximation). The minimum intermolecular distance d was assumed to be 0.35 nm (the wave function is zero at $r<d$) to avoid divergence. The $L=0 \rightarrow 2$ (L is quantum number of angular momentum of the relative motion) scattering term is dominant for this inelastic collision. The author here explains

TABLE I. Listed are molecular rotational constants with $n_v=0$ (B_0), change ratio of the rotational constant by changing n_v [$\eta=(B_{n_v}-B_{n_v+1})/B_0$], permanent dipole moment with $n_v=0$ (μ_0), $n_v=0\rightarrow1$ vibrational transition dipole moment (μ'), $n_v=0\rightarrow1$ transition frequency (f_1), $n_v=0\rightarrow2$ transition frequency (f_2), and the natural linewidth of the $n_v=0\rightarrow1,2$ transitions ($\Delta f_{N1,2}$) are shown. The spectrum is observed using two-photon transition given the probe laser frequency, $f_{1,2}/2$. Superscript "c" denotes calculated values. μ' was estimated using the values of B_0, η, and μ_0 with the method described in Appendix B. Δf_N was estimated using the estimated value of μ'.

	B_0 (GHz)	η	μ_0 (D)	μ' (D)	f_1 (THz)	f_2 (THz)	Δf_{N1} (Hz)	Δf_{N2} (Hz)
^{40}CaH	126.7 [26,27]	0.023 [26]	2.94 [29]	0.42^c	37.8 [26]	74.4 [26]	2.23^c	4.46^c
^{24}MgH	174.5 [26,28]	0.032 [26,28]	1.23^c [30]	0.21^c	42.9 [26,28]	83.9 [26,28]	0.82^c	1.64^c

the details on the calculation procedure in Ref. [31]. Figure 1 plots the elastic- and inelastic-collision cross sections between ^{24}MgH (boson), ^{40}CaH (boson), and ^{15}NH ($^3\Sigma$ $N=0$ state, boson) molecules as a function of the collision kinetic energy. Magnetic field B is 50 G in Fig. 1(a) and 500 G in Fig. 1(b). Krems and Dalgarno expected that inelastic collision would generally be more significant for molecules in the $^3\Sigma$ $N=0$ state than molecules in the $^2\Sigma$ $N=0$ state [18]. The σ_i between ^{24}MgH molecules is actually smaller than that between ^{15}NH molecules by a ratio of 1/3. However, the σ_i between ^{40}CaH molecules is much larger than those between

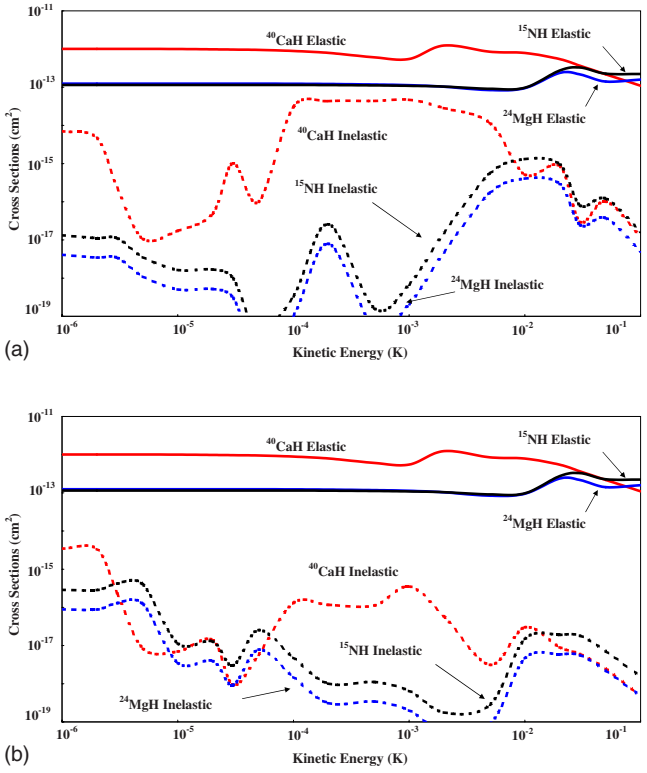

FIG. 1. (Color online) Elastic and inelastic collision cross sections between magnetically trapped ^{40}CaH and ^{24}MgH molecules in $|N=0,J=1/2,F=1,M_F=1\rangle$ state and ^{15}NH molecules in $|N=0,J=1,F_1=3/2,F=2,M_F=2\rangle$ state as functions of collision kinetic energy. Magnetic field is (a) 50 G and (b) 500 G. Solid (dotted) lines denote elastic (inelastic) collision cross sections. Black, red, and blue lines (online) correspond to ^{15}NH, ^{40}CaH, and ^{24}MgH molecules.

^{15}NH or between ^{24}MgH molecules, as Krems also anticipated [32]. This is because the intermolecular attractive force (electric dipole-induced dipole interaction) is much stronger for ^{40}CaH molecules than those for ^{24}MgH and ^{15}NH molecules (larger value of μ_0). Then, magnetic interaction also becomes more significant for ^{40}CaH molecules than for ^{24}MgH and ^{15}NH molecules because of the shorter intermolecular distance.

As B increases, the inelastic collision cross sections increase with ultralow kinetic energy region ($<10^{-4}$ K) and decrease with kinetic energy region higher than 10^{-3} K. This result is explained as follows. The energy discrepancy between $M_S=1/2$ and $-1/2$ states ($\Delta E_{\rm MS}$) is proportional to the magnetic field B (see Sec. III). With ultralow kinetic energy, the distortion of the incident (scattering) wave function is small. Then each incident (scattering) wave function $\phi_L(r)$ is proportional to $k^{L+1}r^L$ at $kr<1$ and each $L\rightarrow L'$ scattering term is proportional to $(k/k')^{2L-1}$, where k and k' are the wave numbers of incident and scattering waves [31]. Considering $k\propto K^{1/2}$ and $k'\propto(K+\Delta E_{\rm MS})^{1/2}$, the $L=0\rightarrow2$ scattering term is proportional to $[(K+\Delta E_{\rm MS})/K]^{1/2}$ and σ_i increases as B becomes higher. With higher kinetic energy, the distortion of $\phi_L(r)$ by the intermolecular attractive force is significant and $\phi_L(r)\propto k^{-L}r^{-(L+1)}$ [31]. Then each $L\rightarrow L'$ scattering term is proportional to $k^{-(2L+3)}k'^{-(2L'+1)}$. The $L=0\rightarrow2$ scattering term is proportional to $K^{-3/2}(K+\Delta E_{\rm MS})^{-5/2}$ and σ_i decreases as B becomes higher.

Considering the ratio of the inelastic-collision cross section to the elastic-collision cross section Q, evaporative cooling easily occurs for ^{24}MgH molecules with any kinetic energy region ($Q\leq10^{-3}$). For ^{40}CaH molecules, as $Q>10^{-2}$ with the kinetic energy region between 10^{-4} K and 10^{-2} K with $B=50$ G, evaporative cooling is more difficult for ^{40}CaH molecules than for ^{24}MgH molecules. When the kinetic energy region is higher than 10^{-2} K, $Q(<10^{-3})$ is almost same order for ^{40}CaH and ^{24}MgH molecules with any value of B (confirmed taking $K/k_B=50$ mK, $B=50,500,1000,2000$, and 3000 G).

When the molecular density is lower than 10^{11} cm^{-3}, $\tau_{\rm th}$ is longer than 10 s.

III. FREQUENCY SHIFT

Figure 2 shows the energy structure of XH molecules in the $^2\Sigma$ state (X: ^{40}Ca or ^{24}Mg). This section discusses the

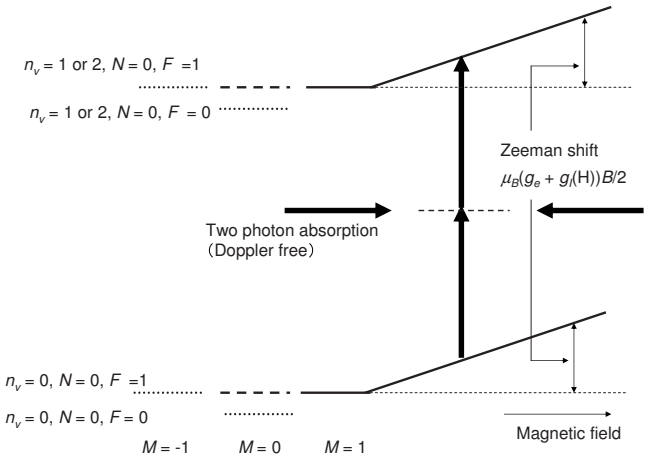

FIG. 2. Energy structure of ^{40}CaH and ^{24}MgH molecules in $^2\Sigma$ $N=0$ state. $(F=1,M=1)$ and $(F=1,M=0)$ are low field seeking states (trapped) and $(F=1,M=-1)$ and $(F=0,M=0)$ states are high field seeking states (not trapped). Zeeman energy shift of molecules in the $(F=1,M=1)$ state is also shown.

shift in the XH $|^2\Sigma,n_v=0,N=0,J=1/2,F=1,M_F=1\rangle \rightarrow |^2\Sigma,n_v=p,N=0,J=1/2,F=1,M_F=1\rangle$ $(p=1,2)$ transition frequencies f_p. The values of f_p, the vibrational transition dipole moment between $n_v=0$ and 1 states μ', and the natural linewidth (Δf_{Np}) of ^{24}MgH or ^{40}CaH molecules are listed in Table I. As shown in Appendix B, μ' was estimated [33] by

$$\mu' = \sqrt{\eta}\mu_0,$$

$$\eta = \frac{B_{n_v} - B_{n_v+1}}{B_0}. \tag{3}$$

The vibrational transition dipole moment $\langle n_v|\mu|n_v-1\rangle$ is given by $\sqrt{n_v}\mu'$.

These transitions are dipole forbidden and can be observed using two-photon absorption by means of two counterpropagating laser lights with a frequency of $f_{1,2}/2$; therefore, the observed spectrum is free from the first order Doppler effect. This section discusses estimates of frequency shifts caused by Zeeman shift (induced by a trapping magnetic field), the second order Doppler effect, ac-Stark shift (induced by the irradiated probe laser and black body radiation), and the collision between trapped molecules.

A. Zeeman shift

The Zeeman shift in transition frequency is caused by the difference in Zeeman energy shifts in upper and lower energy states. First, let us consider the Zeeman energy shift E_Z of trapped molecules, whose energy distribution is thermal equilibrium with temperature T. We assumed that the molecules would only be trapped by the Zeeman trapping force and that the magnetic field would be zero at the trap center. When the magnetic field distribution is given by $B \propto R^{n_B}$, the mean value of E_Z is obtained using the virial law as $2K/n_B = 3k_BT/n_B$ (K is the mean kinetic energy).

The mean Zeeman shift in the $|n_v,C\rangle \rightarrow |n_v',C'\rangle$ $(|C\rangle = |N,J,F_1,F,M_F\rangle)$ transition frequency is given by

$$(\Delta f_Z)_{\mathrm{av}} = \left(\frac{E_Z(n_v',C') - E_Z(n_v,C)}{h}\right)_{\mathrm{av}} = \frac{3k_BT}{hn_B}\left(\frac{E_Z(n_v',C') - E_Z(n_v,C)}{E_Z(n_v,C)}\right)_{\mathrm{av}}. \tag{4}$$

Here, let us consider the dependence of E_Z on the magnetic field and $|n_v,C\rangle$. Assuming pure N states, all $|C\rangle$ states of XH molecules (e.g., X: ^{24}Mg or ^{40}Ca) are described as (X atoms have no nuclear spin)

$$M_F = M_N + M_S + M_{I(\mathrm{H})},$$

$$|C\rangle = \sum \gamma(M_N,M_S,M_{I(\mathrm{H})})|N,M_N,M_S,M_{I(\mathrm{H})}\rangle, \tag{5}$$

and the Zeeman coefficient $Z_{n_v}^{C,\mathrm{pure}}$ $[=(\partial E_Z/\partial B)/h : B$ is magnetic field] is given by

$$Z_{n_v}^{C,\mathrm{pure}} = \mu_B \sum |\gamma(M_N,M_S,M_{I(\mathrm{H})})|^2 \times [g_N M_N + g_S M_S + g_{I(\mathrm{H})} M_{I(\mathrm{H})}], \tag{6}$$

where μ_B is the Bohr magneton and $g_{N,S,I}$ are the g factors for molecular rotation ($g_N < 10^{-3}$ [34]), electron spin ($g_S = 2.003$), and nuclear spin ($g_{I(\mathrm{H})} \approx 3.0 \times 10^{-3}$ [35]), respectively. Generally, $\gamma(M_N,M_S,M_{I(\mathrm{H})})$ depends on the magnetic field and the splitting of hyperfine states; therefore, E_Z is a nonlinear function of B. If hyperfine splitting depends on the vibrational state, Zeeman shift is also significant with pure vibrational-transition frequencies $(|n_v,C\rangle \rightarrow |n_v',C\rangle)$. However, the Zeeman shift in the $|C_a\rangle = |N=0,J=S,F_1=S+I(\mathrm{H}),F=S+I(\mathrm{H}),M_F=S+I(\mathrm{H})\rangle$ state does not depend on hyperfine splitting since

$$|C_a\rangle = |N=0,M_N=0,M_S=S,M_{I(\mathrm{H})}=I(\mathrm{H})\rangle,$$

$$Z_{n_v}^{a,\mathrm{pure}} = \mu_B[g_S S + g_{I(\mathrm{H})} I(\mathrm{H})],$$

$$S = I(\mathrm{H}) = 1/2. \tag{7}$$

The Zeeman energy shift is strictly linear to B for molecules in the $|C_a\rangle$ state (see Fig. 2).

The mean Zeeman shift in the $|n_v,C_a\rangle \rightarrow |n_v',C_a\rangle$ transition frequency is given by

$$(\Delta f_Z)_{\mathrm{av}} = \left(\frac{E_Z(n_v,C)}{h}\right)_{\mathrm{av}} \frac{Z_{n_v'}^{a,\mathrm{pure}} - Z_{n_v}^{a,\mathrm{pure}}}{Z_{n_v}^{a,\mathrm{pure}}} = \frac{3k_BT}{hn_B}\frac{Z_{n_v'}^{a,\mathrm{pure}} - Z_{n_v}^{a,\mathrm{pure}}}{Z_{n_v}^{a,\mathrm{pure}}}. \tag{8}$$

Actually g_S is independent of the vibrational state and $(\Delta f_Z)_{\mathrm{av}}$ is actually very small. Therefore, the $|n_v,C_a\rangle \rightarrow |n_v',C_a\rangle$ transition frequency can be measured without significant Zeeman shift, also when molecules are magnetically trapped. $(\Delta f_Z)_{\mathrm{av}}$ is nonzero because of the slight dependence of g_I on the vibrational state, as explained below. Nuclei

imbedded in the molecules are subject to the magnetic shielding effect and the value of $g_{I(X,\mathrm{H})}$ is slightly different from the value for bare nuclei (chemical shift). The chemical shift σ [$=(g_{I(\mathrm{H})}-g^0_{I(\mathrm{H})})/g^0_{I(\mathrm{H})}$; $g^0_{I(\mathrm{H})}$ is $g_{I(\mathrm{H})}$ for H atom] in each vibrational state is given by [36]

$$\sigma(n_v) = \sigma_0 - \sigma' \frac{r_d(n_v) - r_d(0)}{r_d(0)}. \tag{9}$$

Using $[r_d(n_v)-r_d(0)]/r_d(0)=\eta/2$ (see Appendix B),

$$g_{I(\mathrm{H})}(n_v) - g_{I(\mathrm{H})}(0) = -\frac{\sigma' \eta n_v}{2} g_{I(\mathrm{H})}(0) \tag{10}$$

and

$$\frac{Z^a_{n_v} - Z^a_0}{Z^a_0} \approx -\frac{\sigma' \eta n_v}{2[g_S + g_{I(\mathrm{H})}(0)]} g_{I(\mathrm{H})}(0) \tag{11}$$

are derived. To our knowledge, the values of σ' for ^{40}CaH or ^{24}MgH molecules have not been measured or calculated. Here, let us estimate the Zeeman frequency shift using the value of σ' for HF molecule ($\sigma'=3.7\times10^{-5}$ [36,37]). Assuming a pure $|C_a\rangle$ state, the difference in Zeeman coefficient $Z^a_{1,2}$ from Z^a_0 is given by

$$^{40}\mathrm{CaH} \quad \left|\frac{Z^a_1 - Z^a_0}{Z^a_0}\right| = 5.2\times10^{-10}\left|\frac{Z^a_2 - Z^a_0}{Z^a_0}\right| = 1.04\times10^{-9},$$

$$^{24}\mathrm{MgH} \quad \left|\frac{Z^a_1 - Z^a_0}{Z^a_0}\right| = 7.2\times10^{-10}\left|\frac{Z^a_2 - Z^a_0}{Z^a_0}\right| = 1.44\times10^{-9}. \tag{12}$$

The mean Zeeman shift in the $|n_v=0, C_a\rangle \rightarrow |n_v=1$ or 2, $C_a\rangle$ transition frequency, $(\Delta f^{\mathrm{pure}}_{Z1,2})_{\mathrm{av}}$, is given by

$$^{40}\mathrm{CaH} \quad |\Delta f^{\mathrm{pure}}_{Z1}(\mathrm{Hz})|_{\mathrm{av}} = \frac{3k_BT(Z^a_1 - Z^a_0)}{hn_BZ^a_0} = \frac{33T(\mathrm{K})}{n_B},$$

$$|\Delta f^{\mathrm{pure}}_{Z,2}(\mathrm{Hz})|_{\mathrm{av}} = \frac{66T(\mathrm{K})}{n_B},$$

$$\left|\frac{\Delta f^{\mathrm{pure}}_{Z1,2}}{f_{1,2}}\right|_{\mathrm{av}} = 8.7\times10^{-13}\frac{T(\mathrm{K})}{n_B},$$

$$^{24}\mathrm{MgH} \quad |\Delta f^{\mathrm{pure}}_{Z,1}(\mathrm{Hz})|_{\mathrm{av}} = \frac{45T(\mathrm{K})}{n_B},$$

$$|\Delta f^{\mathrm{pure}}_{Z,2}(\mathrm{Hz})|_{\mathrm{av}} = \frac{90T(\mathrm{K})}{n_B},$$

$$\left|\frac{\Delta f^{\mathrm{pure}}_{Z1,2}}{f_{1,2}}\right|_{\mathrm{av}} = 1.0\times10^{-12}\frac{T(\mathrm{K})}{n_B}. \tag{13}$$

The chemical shift of XH molecule becomes more significant as $|x^X_p - x^{\mathrm{H}}_p|$ increases, where $x^{X,\mathrm{H}}_p$ is the Pauling's electronegativity of X and H atoms. The values of σ' for ^{40}CaH and ^{24}MgH molecules are expected to be smaller than the value for HF molecule (presumably with a factor of 1/2 or 1/3), because $|x^{\mathrm{Ca}}_p - x^{\mathrm{H}}_p|$ and $|x^{\mathrm{Mg}}_p - x^{\mathrm{H}}_p|$ are smaller than $|x^{\mathrm{F}}_p - x^{\mathrm{H}}_p|$ ($x^{\mathrm{H}}_p=2.1$, $x^{\mathrm{F}}_p=4.0$, $x^{\mathrm{Ca}}_p=1.0$, and $x^{\mathrm{Mg}}_p=1.2$). Therefore, the estimate given by Eq. (13) is rather conservative.

The $|C_a\rangle$ state is generally mixed with other rotational states by spin-spin interaction or the electric field, which can make the Zeeman frequency shift more significant than the estimate given by Eq. (13) (see Appendix A). Spin-spin interaction does not exist for molecules in the $^2\Sigma$ state, and the mixture between different N states is only induced by the electric field. When an ac (frequency f_{ac}) or dc ($f_{\mathrm{ac}}=0$) electric field is applied, the $|N,M_N,M_S,M_{I(\mathrm{H})}\rangle=|0,0,1/2,1/2\rangle$ state is mixed with the $|N=1\rangle$ state as indicated by

$$\begin{aligned}|N,M_N,M_S,M_{I(\mathrm{H})}\rangle = |0,0,1/2,1/2\rangle &= |0,0,1/2,1/2\rangle_0 \\ &+ p_{\|}|1,0,1/2,1/2\rangle_0 + p_+|1,1,1/2,1/2\rangle_0 \\ &+ p_-|1,-1,1/2,1/2\rangle_0,\end{aligned}$$

$$p_{\|} = \frac{\mu_{n_v}E_{\|}}{2\sqrt{3}h(2B_{n_v}+f_{\mathrm{ac}})} + \frac{\mu_{n_v}E_{\|}}{2\sqrt{3}h(2B_{n_v}-f_{\mathrm{ac}})},$$

$$p_{\pm} = \frac{\mu_{n_v}E_{\pm}}{2\sqrt{6}h(2B_{n_v}+f_{\mathrm{ac}})} + \frac{\mu_{n_v}E_{\pm}}{2\sqrt{6}h(2B_{n_v}-f_{\mathrm{ac}})}, \tag{14}$$

where the subscript 0 denotes a wave function with a zero-electric field, and $E_{\|}$ represents the electric field components parallel to the direction of the magnetic field. E_+ and E_- are the electric field components rotating right and left on the plane perpendicular to the magnetic field (for a dc electric field, $E_+=E_-$). The Zeeman coefficient of ^{40}CaH and ^{24}MgH molecules in the $|n_v, C_a\rangle$ states under the electric field is approximately given by

$$Z^a_{n_v} = Z^{a,\mathrm{pure}}_{n_v} + Z^{a,\mathrm{mix}}_{n_v},$$

$$Z^{a,\mathrm{pure}}_{n_v} = \frac{1}{2}\mu_B(g_S + g_{I(\mathrm{H})})_{n_v},$$

$$Z^{a,\mathrm{mix}}_{n_v} = \mu_B g_{N,n_v}(p^2_+ - p^2_-)_{n_v}. \tag{15}$$

When a dc electric field is applied, $Z^{a,\mathrm{mix}}_{n_v}=0$ because of $E_+=E_-$ ($p_+=p_-$). The ac-electric field is given by blackbody radiation and the linearly polarized probe laser, where $E_+=E_-$ ($p_+=p_-$) is also satisfied. However, let us also consider the case of $E_+ \gg E_-$ ($p_+ \gg p_-$). Assuming $f_{\mathrm{ac}} \ll B_{n_v}$, $p_+=2\times10^{-5}E(\mathrm{V/cm})$ for ^{40}CaH and $7\times10^{-6}E(\mathrm{V/cm})$ for ^{24}MgH molecules. As the molecular rotation angular velocity is proportional to $\sqrt{B_{n_v}}$, $g_N \propto \sqrt{B_{n_v}}$ and $(g_{N,n_v+1}-g_{N,n_v})/g_{N,n_v} \approx -\eta/2$ are derived. Also considering $(p^2_{+,n_v+1}-p^2_{+,n_v})/p^2_{+,n_v} \approx (B_{n_v}\mu_{n_v+1}/B_{n_v+1}\mu_{n_v})^2 - 1 \approx 3\eta$ (see Appendix B), and $g_N < 10^{-3}$ [34]:

$$^{40}\mathrm{CaH} \quad \left|\frac{Z^{a,\mathrm{mix}}_{n_v+1} - Z^{a,\mathrm{mix}}_{n_v}}{Z^{a,\mathrm{pure}}_{n_v}}\right| = |g_{N,n_v+1}p^2_{+,n_v+1} - g_{N,n_v}p^2_{+,n_v}| < 2.3\times10^{-14}E^2_+(\mathrm{V/cm})^2,$$

$$\left|\frac{\Delta f^{\rm mix}_{Z1,2}}{f_{Z1,2}}\right|_{\rm av} < 1.2\times 10^{-17} E_+^2({\rm V/cm})^2 \frac{T({\rm K})}{n_B},$$

$$(\Delta f_Z)^{\rm mix}_{\rm av} = \frac{3k_B T}{hn_B}\frac{Z^{a,{\rm mix}}_{n_v'} - Z^{a,{\rm mix}}_{n_v}}{Z^{a,{\rm pure}}_{n_v}},$$

$$^{24}{\rm MgH} \quad \left|\frac{Z^{a,{\rm mix}}_{n_v+1} - Z^{a,{\rm mix}}_{n_v}}{Z^{a,{\rm pure}}_{n_v}}\right| < 4\times 10^{-15} E_+^2({\rm V/cm})^2,$$

$$\left|\frac{\Delta f^{\rm mix}_{Z1,2}}{f_{Z1,2}}\right|_{\rm av} < 2\times 10^{-18} E_+^2({\rm V/cm})^2 \frac{T({\rm K})}{n_B}. \quad (16)$$

When $f_{\rm ac} \gg 2B_{n_v}$, $|\Delta f^{\rm mix}_{Z1,2}/f_{Z1,2}|$ becomes smaller than the estimate given by Eq. (16) with a factor of $(2B_{n_v}/f_{\rm ac})^2$. Actually the electric field is much lower than 100 V/cm and $\Delta f^{\rm mix}_{Z1,2} \ll \Delta f^{\rm pure}_{Z1,2}$.

Here we considered the case where molecules are trapped by an anti-Helmholz coil. To reduce $|\Delta f_{Z1,2}/f_{Z1,2}|$ lower than 10^{-15} with this situation, the molecular temperature should be reduced down to 3 mK by evaporative or adiabatic cooling.

The Zeeman frequency shift is much more significant for the ^{14}NH $|X\,^3\Sigma, n_v=0, N=0, J=1, F_1=3/2, F=5/2, M_F=5/2\rangle \rightarrow |X\,^3\Sigma, n_v=1, N=0, J=1, F_1=3/2, F=5/2, M_F=5/2\rangle$ transition, because of the mixture between $(N=0, M_S=1)$ and $(N=2, M_S=\pm 1, 0)$ states induced by the spin-spin interaction (see Appendix A).

B. Second order Doppler effect

When ^{40}CaH and ^{24}MgH molecules are cooled down to 10 mK, their velocities v are on the order of 2 m/s and 2.8 m/s, respectively. The second order Doppler shift is given by

$$\Delta f^{\rm SD}_{1,2} = -\left(\frac{v^2}{2c^2}\right) f_{1,2} \quad (17)$$

and $|\Delta f^{\rm SD}_{1,2}/f_{1,2}| \le 4\times 10^{-17}$.

C. ac Stark effect

When an ac electric field is applied, Stark energy shifts in $|n_v, N=0\rangle$ states are induced by coupling with the $|n_v, N=1\rangle$ and $|n_v \pm 1, N=1\rangle$ states. The off-diagonal matrix elements of the dipole moment are $\langle n_v, N=0|\mu|n_v, N=1\rangle = \mu_{n_v}/\sqrt{3}$, $\langle n_v, N=0|\mu|n_v+1, N=1\rangle \approx \sqrt{n_v+1}\mu'/\sqrt{3}$, and $\langle n_v, N=0|\mu|n_v-1, N=1\rangle \approx \sqrt{n_v}\mu'/\sqrt{3}$. The Stark energy shifts in $|n_v, N=0\rangle$ states, $E_S(n_v)$, are then given by Ref. [38] as

$$E_S(0) = -\frac{2B_0\mu_0^2E^2}{3h(4B_0^2 - f_{\rm ac}^2)} - \frac{(f_1+2B_1)\mu'^2E^2}{3h[(f_1+2B_1)^2 - f_{\rm ac}^2]},$$

$$E_S(1) = -\frac{2B_1\mu_1^2E^2}{3h(4B_1^2 - f_{\rm ac}^2)} + \frac{(f_1-2B_0)\mu'^2E^2}{3h[(f_1-2B_0)^2 - f_{\rm ac}^2]} - \frac{2(f_2-f_1+2B_2)\mu'^2E^2}{3h[(f_2-f_1+2B_2)^2 - f_{\rm ac}^2]},$$

$$E_S(2) = -\frac{2B_2\mu_2^2E^2}{3h(4B_2^2 - f_{\rm ac}^2)} + \frac{2(f_2-f_1-2B_1)\mu'^2E^2}{3h[(f_2-f_1-2B_1)^2 - f_{\rm ac}^2]} - \frac{(f_3-f_2+2B_3)\mu'^2E^2}{h[(f_3-f_2+2B_3)^2 - f_{\rm ac}^2]}, \quad (18)$$

where $f_{\rm ac}$ is the frequency of the ac-electric field, B_3 is the rotational constant in the $n_v=3$ state, and f_3 is the $n_v=0 \rightarrow 3$ transition frequency.

The ac electric field is given by blackbody radiation and the probing laser light.

1. Blackbody radiation

For blackbody radiation, $f_{\rm ac} < f_1$, when the temperature of chamber T_C is lower than 300 K. Here we use approximations $(f_1 \pm 2B_1) \approx (f_2 - f_1 \pm 2B_{1,2}) \approx (f_3 - f_2 + 2B_3) \approx f_1$. The Stark shifts in f_1 and f_2 caused by blackbody radiation $(\Delta f_{\rm BB1}, \Delta f_{\rm BB2})$ are given by

$$\Delta f_{\rm BB1} \approx \frac{2(2f_1-f_2)\mu'^2E^2}{3h^2(f_1^2 - f_{\rm ac}^2)} + \frac{2B_0\mu_0^2E^2}{3h^2(4B_0^2 - f_{\rm ac}^2)} - \frac{2B_1\mu_1^2E^2}{3h^2(4B_1^2 - f_{\rm ac}^2)},$$

$$\Delta f_{\rm BB2} \approx \frac{(5f_2-3f_3-f_1)\mu'^2E^2}{3h^2(f_1^2 - f_{\rm ac}^2)} + \frac{2B_0\mu_0^2E^2}{3h^2(4B_0^2 - f_{\rm ac}^2)} - \frac{2B_2\mu_2^2E^2}{3h^2(4B_2^2 - f_{\rm ac}^2)}. \quad (19)$$

The average wavelength of blackbody radiation is 18 μm (1.8×10^{13} Hz) when $T_C \approx 300$ K [39], and the first term of Eq. (19) is dominant. The average quadratic electric field strength of blackbody radiation is given by 69.2 $({\rm V/cm})^2$ $[T_C({\rm K})/300]^4$. The values of blackbody radiation shift are obtained as

$$^{40}{\rm CaH} \quad \Delta f_{\rm BB1} \approx 7.35\times 10^{-4}{\rm Hz},$$

$$\Delta f_{\rm BB2} \approx 2.94\times 10^{-3}{\rm Hz},$$

$$\Delta f_{\rm BB1}/f_1 \approx 1.9\times 10^{-17},$$

$$\Delta f_{\rm BB2}/f_2 \approx 3.8\times 10^{-17},$$

$$^{24}{\rm MgH} \quad \Delta f_{\rm BB1} \approx 2.1\times 10^{-4}{\rm Hz},$$

$$\Delta f_{\rm BB2} \approx 8.4\times 10^{-4}{\rm Hz},$$

$$\Delta f_{\rm BB1}/f_1 \approx 4.9\times 10^{-18},$$

$$\Delta f_{\rm BB2}/f_2 \approx 9.8\times 10^{-18}. \quad (20)$$

Molecules are actually trapped inside the cryogenic chamber ($T_C < 1$ K) [19] and the average of $f_{\rm ac}$ is lower than 5×10^{10} Hz. Therefore, the first term of Eq. (19) is negligibly small in comparison with the other two terms. The quadratic electric field strength of blackbody radiation is less than 8.6×10^{-9} $({\rm V/cm})^2$ and the Stark shift caused by blackbody radiation is less than 1.7×10^{-9} Hz.

2. Light shift

(*a*) $n_v=0\rightarrow 1$ *transition.* When $n_v=0\rightarrow 1$ transition is observed, $f_{ac}=f_1/2(\gg B_0)$ and the light shift, Δf_{L1}, which is then approximately given by

$$\Delta f_{L1} \approx \frac{8(2f_1-f_2)\mu'^2E^2}{9h^2f_1^2}. \tag{21}$$

A typical value of E (E_{sat}), where the two-photon-transition rate has the same value as the spontaneous emission rate from the $n_v=1$ state $2\pi\Delta f_{N1}$, is estimated as

$$\frac{2\pi\langle n_v=0,N=0|\mu|n_v=0,N=1\rangle\langle n_v=0,N=1|\mu|n_v=1,N=0\rangle}{h^2(f_1/2-2B_0)}E_{sat}^2=2\pi\Delta f_{N1},$$

$$E_{sat}^2=\frac{3h^2f_1\Delta f_{N1}}{2\mu_0\mu'}. \tag{22}$$

Using Eq. (22), Eq. (21) can be rewritten as

$$\Delta f_{L1} \approx \frac{4\mu'(2f_1-f_2)\Delta f_{N1}}{3\mu_0 f_1}\left(\frac{E}{E_{sat}}\right)^2=\frac{4\mu'(2f_1-f_2)\Delta f_{N1}}{3\mu_0 f_1}\frac{I}{I_S}. \tag{23}$$

Here, I is the power density of the probe laser light and I_S (listed in Table II) is the saturation power density. Δf_{L1} is reduced taking lower value of I/I_S. When $E=E_{sat}$, $\Delta f_{L1}=6.7$ (4.2) mHz and $\Delta f_{L1}/f_1=1.7\times10^{-16}$ (9.8×10^{-17}) for ^{40}CaH (^{24}MgH) molecules. The light shift is negligible small, also when the power of the probe laser light is high enough to obtain a high S/N ratio.

(*b*) $n_v=0\rightarrow 2$ *transition*. When $n_v=0\rightarrow 2$ transition is observed, $f_{ac}=f_2/2$ ($\gg B_0$) and the light shift, Δf_{L2}, which is approximately given by

$$\Delta f_{L1} \approx -\frac{\mu'^2E^2}{h^2}\left[\frac{1}{2f_3-3f_2+4B_3}-\frac{1}{3f_2-6f_1-12B_1}\right]$$

using $2f_3-3f_2=3f_2-6f_1$ (second term of vibrational energy) and $B_0\approx B_1\approx B_3$

$$\approx\frac{4}{9}\frac{\mu'^2E^2}{h^2}\frac{B_0}{(f_1-f_2/2)^2}. \tag{24}$$

A typical value of E (E_{sat}), where the two-photon-transition rate has the same value as the spontaneous emission rate from the $n_v=2$ state $2\pi\Delta f_{N2}$, is estimated as

$$\frac{2\pi\langle n_v=0,N=0|\mu|n_v=1,N=1\rangle\langle n_v=1,N=1|\mu|n_v=2,N=0\rangle}{h^2(f_1-f_2/2)}E_{sat}^2=2\pi\Delta f_{N2},$$

$$E_{sat}^2=\frac{3h^2(f_1-f_2/2)}{\sqrt{2}\mu'^2}\Delta f_{N2}. \tag{25}$$

TABLE II. Listed are the wavelength (λ_{probe}) and saturation power density (I_s) of the probe laser, the wavelength of the pump laser (λ_d), and the wavelength of observed fluorescence (λ_f) are shown.

		λ_{probe} (μm)	I_s (W/cm^2)	λ_d (nm)	λ_f (nm)
^{24}MgH	$n_v=0\rightarrow 1$	14.02	2.2	478 [26]	446 [26]
	$n_v=0\rightarrow 2$	7.15	0.89	493 [26]	459 [26]
^{40}CaH	$n_v=0\rightarrow 1$	15.87	1.1	691 [26]	634 [26]
	$n_v=0\rightarrow 2$	8.06	0.34	692 [26]	635 [26]

Using Eq. (25), Eq. (24) can be rewritten as

$$\Delta f_{L1} \approx \frac{4B_0\Delta f_{N2}}{3\sqrt{2}(f_1-f_2/2)}\left(\frac{E}{E_{sat}}\right)^2=\frac{4B_0\Delta f_{N2}}{3\sqrt{2}(f_1-f_2/2)}\frac{I}{I_S}. \tag{26}$$

Δf_{L2} is reduced taking a lower value of I/I_S. When $I=I_S$, $\Delta f_{L1}=0.88$ (0.28) Hz and $\Delta f_{L2}/f_2=1.2\times10^{-14}$ (3.4×10^{-15}) for ^{40}CaH (^{24}MgH) molecules. To reduce $\Delta f_{L2}/f_2$ lower than 10^{-15}, I/I_S should be lower than 0.1 (0.3) for ^{40}CaH (^{24}MgH) molecules. The fraction of molecules excited to the $n_v=2$

state is on the order of $(I/I_S)^2$. Therefore, the laser power density should be chosen with a trade off between low light shift and a high S/N ratio.

D. Collision shift

When molecules get close to other molecules, intermolecular interaction causes energy shift E_c. The collision shift of $f_{1,2}$ ($\Delta f_{C1,2}$) is caused by the difference in E_c in the vibrational ground and excited states.

The collision shift is

$$\Delta f_{C1,2} = nv\sigma_{1,2}, \tag{27}$$

where n denotes the molecular density, v is the mean relative velocity, and $\sigma_{1,2}$ represents the cross sections of the collision shift. Collision partner molecules are mostly in the $|n_v=0,N=0\rangle$ state. Intermolecular interaction is actually dominated by electric dipole-induced dipole interaction, as described in Sec. II. The $\sigma_{1,2}$ for ^{40}CaH and ^{24}MgH molecules (bosons) are given by [16] as

$$\sigma_{1,2} = \frac{4\pi}{k^2}\sum_{L=\text{even}}(2L+1)\frac{\chi_{1,2}}{|\chi_{1,2}|}\frac{2\gamma_L k^{2L+1}}{1+\gamma_L^2 k^{4L+2}},$$

$$\gamma_{L=0} = \left(\frac{m|\chi_{1,2}|}{8\hbar^2}\right)^{1/4}\frac{\Gamma(3/4)}{\Gamma(5/4)},$$

$$\gamma_{L\geq 1} = \frac{L}{(L+1)(2L-1)!!(2L+1)!!}\left[\frac{6m|\chi_{1,2}|}{\hbar^2 L(L+1)}\right]^{(2L+1)/4},$$

$$\chi_{1,2} = \frac{\mu_0^2}{96\pi^2\varepsilon_0^2 h}\left(\frac{\mu_0^2}{B_0}-\frac{\mu_{1,2}^2}{B_1}\right)(1+3\cos^2\xi),$$

using $\mu_{n_v}^2=(1+n_v\eta)\mu_{n_v}^2$ and $B_{n_v}=(1-n_v\eta)B_0$ (see Appendix B)

$$\chi_1 \approx -\frac{\mu_0^4}{48\pi^2\varepsilon_0^2 hB_0}\eta(1+3\cos^2\xi),$$

$$\chi_2 \approx -\frac{\mu_0^4}{24\pi^2\varepsilon_0^2 hB_0}\eta(1+3\cos^2\xi),$$

$$k = \frac{2\pi mv}{h}, \tag{28}$$

where ξ is the angle between the vectors of the dipole moment and the molecular relative position and m is the reduced mass. When the collision kinetic energy, K/k_B, is lower than 10 mK, the collision cross section is mostly dominated by the $L=0$ scattering term and σ_s is inversely proportional to v. Therefore, $\Delta f_{C1,2}$ does not depend on K and $\Delta f_{C1}/n$ and $\Delta f_{C2}/n$ are roughly estimated to be on the order of -2.4×10^{-12} and -4.8×10^{-12} (-1.7×10^{-13} and -3.4×10^{-13}) Hz cm^3 for ^{40}CaH (^{24}MgH)molecules at $K/k_B<10$ mK. Taking $n<10^9/\text{cm}^3$, $\Delta f_{C1,2}/f_{1,2}$ is smaller than $10^{-16}(10^{-17})$ for ^{40}CaH (^{24}MgH) molecular transition.

IV. EXPERIMENTAL PROCEDURE

The transition frequency should be measured using the following procedure.

(1) XH molecules are produced by the laser ablation of XH_2 (X: ^{24}Mg or ^{40}Ca). Weinstein *et al.* produced more than 10^{10} ^{40}CaH molecules [19].

(2) XH molecules in the $M_S=1/2$ state are loaded into the magnetic trap area after cooling with buffer gas. The magnetic field distribution is given by $B(R)=PR^{n_B}$. This loading takes about 0.4 s. The buffer gas should be quickly extracted out (<0.1 s), opening a gate to another chamber. More than 10^8 molecules are expected to be trapped [19].

(3) The molecular temperature should be reduced using evaporative cooling. Irradiating a microwave with frequency f_{ev}, molecules with energies higher than $E_{\max}=h\mu_B f_{\text{ev}}/2$ are transformed to the $M_S=-1/2$ state and repelled from the trap. The mean trapping energy is $E_{\max}/2$ and the fraction $(E_{\max}/k_BT_{\text{in}})$ of initially trapped molecules remain in the trapping region (selection of low energy molecules). The mean Zeeman potential energy is $(E_Z)_{\text{av}}^{\text{noneq}}=E_{\max}/(n_B+2)$ [see Eq. (2)].

The mean Zeeman potential energy is further reduced with a procedure where the energy distribution is transformed to the Boltzmann distribution with a temperature T_{eq} ($\approx E_{\max}/10k_B$ [22]). The final value of mean three-dimensional Zeeman potential energy is in the order of $(E_Z)_{\text{av}}^{\text{ev}}=3k_BT_{\text{eq}}/n_B\approx 3E_{\max}/10n_B$. When $E_{\max}$ is initially taken higher than k_BT_{in} and reduced slowly down to the final value $E_{\max}^f$ (taking longer time than τ_{th}), the number of trapped molecules at the end of this procedure is much larger than $(E_{\max}^f/k_BT_{\text{in}})$ (evaporative cooling).

(4) The magnetic gradient is adiabatically reduced ($P=P_i\rightarrow P_fP_i>P_f$), so that the molecular trapping energy E_{trap} (=kinetic energy +Zeeman potential energy) is reduced with a factor of $(P_f/P_i)^{2/(n_B+2)}$ (adiabatic cooling). The molecular density is also reduced down to the value, where the collision shift is negligible small ($<10^9/\text{cm}^3$). This procedure should take about 0.1 s, that is much longer than the period of molecular vibrational motion inside the trap area (in the order of 1 ms).

(5) Molecules in vibrationally excited states are transformed to the ground state, irradiating the pump laser (resonant with the $|X\,^2\Sigma, n_v=1 \text{ or } 2\rangle\rightarrow|B\,^2\Sigma, n_v=0 \text{ or } 1\rangle$ transition) for a few μs. The wavelength of pump lasers are listed in Table II. The pump-laser power density is higher than 1 mW/cm^2 and the irradiating time is in the order of 10 μs. It is preferable to use this procedure to improve the S/N ratio, because $10^{-1}-10^{-2}$ of trapped molecules are initially in the $n_v=1$ or 2 states [19].

(6) The IR probe laser is irradiated to counterpropagate in two directions for a period longer than $\tau\approx 1/2\pi\Delta f_{N1,2}$. The wavelengths of probe laser ($\lambda_p=2c/f_{1,2}$) are listed in Table II. The power density of the probe laser I should be lower than the saturation power density (I_s: listed in Table II), so that the light shift of the transition frequency is lower than 10^{-15}.

(7) The pump laser is irradiated again to induce the $|X\,^2\Sigma, n_v=1\rangle\rightarrow|B\,^2\Sigma, n_v=0\rangle$ (or $|X\,^2\Sigma, n_v=2\rangle\rightarrow|B\,^2\Sigma, n_v$

$=1\rangle$) transition. The pump-laser power density is higher than 1 mW/cm^2 and the irradiating time is in the order of 10 μs. Frequency shifted fluorescence $|B\,^2\Sigma, n_v=0\rangle \rightarrow |X\,^2\Sigma, n_v=0\rangle$ (or $|B\,^2\Sigma, n_v=1\rangle \rightarrow |X\,^2\Sigma, n_v=1\rangle$) is detected. The wavelengths of observed fluorescence are shown in Table II.

The frequency uncertainty is dominated by the mean Zeeman frequency shift, which is proportional to the mean Zeeman potential energy [see Eq. (8)]. When the mean Zeeman potential energy is $3\times n_B$ mK (temperature$1\times n_B$ mK), the uncertainty of observed frequency is lower than 10^{-15} [see Eqs. (8) and (13)]. Weinstein *et al.* reduced the temperature of magnetically trapped Cr atoms (initial density 10^{11} cm^3) from 1 K down to 10 mK, using evaporative and adiabatic cooling [21]. ^{24}MgH and ^{40}CaH molecules are in principle much more advantageous for evaporative cooling than Cr atoms, because the ratio of the inelastic collision cross section to the elastic collision cross section Q is much smaller than that for Cr atoms (for Cr atoms, $Q>1$ with kinetic energy lower than 10 mK and $Q\approx 1/10$ with kinetic energy between 50–200 mK) [21]. However, the initial density of ^{40}CaH molecule is presently so low as 8×10^7 cm^3 [19] and evaporative cooling takes time longer than 10^4 s (3 h). When the molecular density at procedure (2) is higher than 10^{11} cm^3, evaporative cooling is possible within 10 s. The initial molecular density can be increased by (i) giving higher magnetic field gradient and (ii) producing XH molecules at a position close to the trap center.

Here we consider the possibility to reduce the mean Zeeman potential energy without evaporative cooling. The mean Zeeman potential energy is reduced also by the adiabatic cooling effect at procedure (4). We assume $n_B=1$ (trapped by anti-Helmholz coil). When the Zeeman potential depth is adiabatically reduced from 2 K down to 9 mK, $E_{\rm trap}$ is reduced with a factor of 0.027 [$=(9/2000)^{2/3}$] and molecules, whose initial value of $E_{\rm trap}/k_B$ is lower than 330 mK, remain in the trap after procedure (4). Assuming that the initial temperature is 200 mK (mean value of $E_{\rm trap}/k_B$ is 900 mK), 18% of initially trapped molecules remain in the trap. The mean Zeeman potential energy after procedure (4) is 3 mK and the Zeeman frequency shift is lower than 10^{-15}. Therefore, the measurement with the frequency uncertainty lower than 10^{-15} is possible also without evaporative cooling.

Here we consider the frequency stability without evaporative cooling. The expected frequency stability is estimated by the Allan variance [40]:

$$\sigma_y = \frac{\Delta f}{\pi f_{1,2}}\frac{1}{\sqrt{N_d}}\sqrt{\frac{\tau_e}{\tau}}, \tag{29}$$

where N_d is number of detected molecules, τ_e is the time for one measurement cycle and τ is the measurement time. Without evaporative cooling, τ_e is in the order of 1 s. N_d is estimated as follows. The number of trapped molecules after procedure (4) is larger than 10^7 molecule). Assuming also $(I/I_S)\geq 10^{-1}$, more than 10^5 molecules are transformed to the vibrational excited state. The S/N ratio is then on the same order with an ^{87}Sr lattice clock using 10^4 atoms [41] because the two-photon spectrum is free from the first order Doppler effect and 1/4 of all molecules (1/2 of trapped molecules) are in the $|n_v=0, N=0, J=1/2, F=1, M_F=1\rangle$ state. The instability of ^{24}MgH $n_v=0\rightarrow 2$ transition frequency is on the order of $3\times 10^{-16}/\sqrt{\tau\,(\rm s)}$, taking $N_d=10^5$ and $\tau_e=1$ s.

When the initial molecular density is increased up to 10^{11} cm^3 and evaporative cooling is performed within 10 s, the frequency stability is improved because of the larger value of N_d (although τ_e becomes on the order of 10 s).

V. CONCLUSION

The $|n_v=0, N=0, J=1/2, F=1, M_F=1\rangle \rightarrow |n_v=1$ or $2, N=0, J=1/2, F=1, M_F=1\rangle$ transition frequencies of magnetically trapped molecules in the $^2\Sigma$ state are useful for observing variations in the electron-to-proton mass ratio, mainly because of small Zeeman frequency shift. The uncertainty of observed transition is sufficiently low (10^{-15}) to measure variations in an electron-to-proton mass ratio in a laboratory.

^{24}MgH molecules are more advantageous than ^{40}CaH molecules for trapping and evaporative cooling, because of their smaller inelastic-collision cross sections. Also note that collisional frequency shift and light shift in ^{24}MgH transition are smaller than those in ^{40}CaH transition. Therefore, ^{24}MgH transition is more advantageous for precise measurement than ^{40}CaH molecules. ^{24}MgH transition is more advantageous than ^{40}CaH transition to also obtain a high S/N ratio because of the shorter wavelength (larger photon energy) of observed fluorescence.

APPENDIX A

This appendix estimates the Zeeman frequency shift of the ^{14}NH $|X\,^3\Sigma, n_v=0, N=0, J=1, F_1=3/2, F=5/2, M_F=5/2\rangle \rightarrow |X\,^3\Sigma, n_v=1, N=0, J=1, F_1=3/2, F=5/2, M_F=5/2\rangle$ transition.

Spin-spin interaction is significant for molecules in the $^3\Sigma$ state, for example ^{14}NH molecules. Because of this interaction, the $|N=0, M_N=0, M_S=1\rangle$ state is mixed with the $|N=2, M_N=0, M_S=1\rangle$, $|N=2, M_N=1, M_S=0\rangle$ and $|N=2, M_N=2, M_S=-1\rangle$ states [18]. The mix can roughly be estimated by $s_{n_v}=\lambda/6B_{n_v}$, where λ is the spin-spin interaction parameter in the n_vth vibrational state. Taking $\lambda=27$ GHz and $B_0=490$ GHz in the vibrational ground state [42], $s_0\approx 0.009$. As $B_{n_v}[=B_0(1-n_v\eta)]$ depends on the vibrational state, s also depends on the vibrational state. Taking $\eta=0.039$ [26],

$$\frac{Z^a_{n_v}-Z^a_0}{Z^a_0}=(s_0^2-s_{n_v}^2),$$

$$(\Delta f_Z^{\rm mix})_{\rm av}\approx\frac{3k_BT(s_0^2-s_{1,2}^2)}{hn_B},$$

$$s_1^2-s_0^2=\frac{B_1^{-2}-B_0^{-2}}{B_0^{-2}}s_0^2\approx 2\eta s_0^2=6.3\times 10^{-6},$$

$$(\Delta f_{Z,1}^{\rm mix})_{\rm av}({\rm Hz})\approx -3.9\times 10^5\frac{T({\rm K})}{n_B},$$

$$s_2^2 - s_0^2 \approx 4\eta s_0^2 = 1.3 \times 10^{-5},$$

$$(\Delta f_{Z,2}^{\mathrm{mix}})_{\mathrm{av}}(\mathrm{Hz}) \approx -7.8 \times 10^5 \frac{T(\mathrm{K})}{n_B}.$$

The $|\Delta f_Z^{\mathrm{mix}}|_{\mathrm{av}}$ is much larger than $|\Delta f_Z^{\mathrm{pure}}|_{\mathrm{av}}$ and $|\Delta f_{Z1,2}/f_{1,2}|_{\mathrm{av}} \approx 3.9 \times 10^{-9} T(\mathrm{K})/n_B$. Assuming $T \approx 1$ mK and $n_B = 1$ (trapped by anti-Helmholz coil), $|\Delta f_Z/f|_{\mathrm{av}}$ is on the order of 3.9×10^{-12}.

APPENDIX B

This appendix estimates the internuclear distance, permanent dipole moment, and vibrational transition dipole moment of a diatomic molecule, XY, in all vibrational states (n_v) using a parameter $\eta[=(B_{n_v} - B_{n_v+1})/B_0]$.

When X and Y atoms have electric charge $\pm q$, dipole moment of XY molecule is given by

$$\mu = q r_d,$$

where r_d is relative position between two nuclei. The dipole matrix element is given by

$$\mu_{n_v} = \langle n_v | \mu | n_v \rangle = q r_d(n_v),$$

$$\langle n_v | \mu | n_v - 1 \rangle = \sqrt{n_v}\mu',$$

$$\mu' = q(\Delta r)_0,$$

$$(\Delta r)_0 = \langle 1 | r_d | 0 \rangle = \frac{1}{2\pi}\sqrt{\frac{h}{2 m_{XY} f_1}},$$

where m_{XY} is the reduced mass between X and Y atoms and $r_d(n_v)$ is the mean value of r_d in each vibrational state. The value of $r_d(n_v)$ is given by

$$r_d^2(n_v) = r_d^2(0) + n_v(\Delta r)_0^2.$$

Considering $B_{n_v} = \hbar^2/2 m_{\mathrm{XY}} r_d(n_v)^2$, the following formulas using $\eta[=(B_{n_v} - B_{n_v+1})/B_0]$ (see Table I) are derived as

$$\eta = \frac{r_d^{-2}(n_v) - r_d^{-2}(n_v+1)}{r_d^{-2}(n_v)} = 1 - \left[\frac{r_d^2(n_v)}{r_d^2(n_v+1)}\right].$$

As can be seen from Table I, $\eta \ll 1$ and the following approximations are valid:

$$(\Delta r)_0^2 = \left(\frac{1}{1-\eta} - 1\right) r_d^2(0) \approx \eta r_d^2(0),$$

$$\frac{r_d(n_v) - r_d(0)}{r_d(0)} = \sqrt{1 + n_v \eta \left(\frac{(\Delta r)_0}{r_d(0)}\right)^2} - 1 \approx \frac{n_v \eta}{2},$$

$$\frac{\mu_{n_v}^2 - \mu_0^2}{\mu_0^2} = n_v \eta.$$

[1] W. J. Marciano, Phys. Rev. Lett. **52**, 489 (1984); X. Calmet and H. Fritzsch, Eur. Phys. J. C **24**, 639 (2002); P. Langacker, G. Segre, and M. J. Strassler, Phys. Lett. B **528**, 121 (2002); J-P. Uzam, Rev. Mod. Phys. **75**, 403 (2003).

[2] J. K. Webb, M. T. Murphy, V. V. Flambaum, V. A. Dzuba, J. D. Barrow, C. W. Churchill, J. X. Prochaska, and A. M. Wolfe, Phys. Rev. Lett. **87**, 091301 (2001).

[3] E. Reinhold, R. Buning, U. Hollenstein, A. Ivanchik, P. Petitjean, and W. Ubachs, Phys. Rev. Lett. **96**, 151101 (2006).

[4] T. P. Heavner, S. R. Jefferts, E. A. Donley, J. H. Shirley, and T. E. Parker, Metrologia **42**, 411 (2005).

[5] W. H. Oskay, S. A. Diddams, E. A. Donley, T. M. Fortier, T. P. Heavner, L. Hollberg, W. M. Itano, S. R. Jefferts, M. J. Delaney, K. Kim, F. Levi, T. E. Parker, and J. C. Bergquist, Phys. Rev. Lett. **97**, 020801 (2006).

[6] T. Schneider, E. Peik, and Chr. Tamm, Phys. Rev. Lett., **94**, 230801 (2005).

[7] H. S. Margolis, G. P. Barwood, G. Huang, H. A. Klein, S. N. Nea, K. Szymaniec, and P. Gill, Science **306**, 1355 (2004).

[8] M. M. Boyd, A. D. Ludlow, S. Blatt, S. M. Foreman, T. Ido, T. Zelevinsky, and J. Ye, Phys. Rev. Lett. **98**, 083002 (2007).

[9] E. Peik, B. Lipphardt, H. Schnatz, T. Schneider, C. Tamm, and S. G. Karshenboim, Phys. Rev. Lett. **93**, 170801 (2004).

[10] E. R. Hudson, H. J. Lewandowski, B. C. Sawyer, and J. Ye, Phys. Rev. Lett. **96**, 143004 (2006).

[11] X. Calmet and H. Fritzsch, Eur. Phys. J. C **24**, 639 (2002).

[12] S. Schiller and V. Korobov, Phys. Rev. A **71**, 032505 (2005).

[13] R. Felder, Metrologia **42**, 323 (2002).

[14] B. Roth, J. C. J. Koelemeij, H. Daerr, and S. Schiller, Phys. Rev. A **74**, 040501(R) (2006).

[15] J. van Veldhoven, R. T. Jongma, B. Sartakov, W. A. Bongers, and G. Meijer, Phys. Rev. A **66**, 032501 (2002); J. van Veldhoven, J. Kuepper, H. L. Bethlem, B. Sartakov, A. J. A. van Roji, and G. Meijer, Eur. Phys. J. D **31**, 337 (2004).

[16] M. Kajita, Phys. Rev. A **74**, 035403 (2006).

[17] D. Egorov, W. C. Campbell, B. Friedrich, S. E. Maxwell, E. Tsikata, L. D. van Buuren, and J. M. Doyle, Eur. Phys. J. D **31**, 307 (2004).

[18] R. V. Krems and A. Dalgarno, J. Chem. Phys. **120**, 2296 (2004).

[19] J. D. Weinstein, R. deCarvalho, T. Guillet, B. Friedrich, and J. M. Doyle, Nature (London) **395**, 148 (1998).

[20] D. G. Fried, Thomas C. Killian, L. Willmann, D. Landhuis, S. C. Moss, D. Kleppner, and T. J. Greytak, Phys. Rev. Lett. **81**, 3811 (1998).

[21] J. D. Weinstein, R. deCarvalho, C. I. Hancox, and J. M. Doyle, Phys. Rev. A **65**, 021604(R) (2002).

[22] M. Yamashita, M. Koashi, and N. Imoto, Phys. Rev. A **59**, 2243 (1999).

[23] C. R. Monroe, E. A. Cornell, C. A. Sackett, C. J. Myatt, and C. E. Wieman, Phys. Rev. Lett. **70**, 414 (1993).

[24] S. Hoekstra, J. J. Gilijamse, B. Sartakov, N. Vanhaecke, L. Scharfenberg, S. Y. T. van de Meerakker, and G. Meijer, Phys. Rev. Lett. **98**, 133001 (2007).

[25] M. Kajita, T. Suzuki, H. Odashima, Y. Moriwaki, and M. Tachikawa, Jpn. J. Appl. Phys., Part 2 **40**, L1260 (2001).
[26] http://webbook.nist.gov/chemistry/
[27] C. I. Frum, J. J. Oh, E. A. Cohen, and H. M. Pickett, Astrophys. J. Lett. **408**, L61 (1999).
[28] L. Wallace, K. Hinkle, G. Li, and P. Bernath, Astrophys. J. **524**, 454 (1999).
[29] T. C. Steimle, J. Chen, and J. Gengler, J. Chem. Phys. **121**, 829 (2004).
[30] W. Meyer and P. Rosmus, J. Chem. Phys. **63**, 2356 (1975).
[31] M. Kajita, Phys. Rev. A **74**, 032710 (2006).
[32] R. V. Krems (private communication).
[33] T. Leininger and G. Jeung, J. Chem. Phys. **103**, 3942 (1995).
[34] C. H. Townes and A. L. Schawlow, *Microwave Spectroscopy* (McGraw-Hill Book Company, New York, 1955), p. 290.
[35] J. Vanier and C. Audoin, *The Quantum Physics of Atomic Frequency Standards* (Adam Hilger, Bristol and Philadelphia, 1989), p. 24.
[36] B. Cromp, T. Carrington, D. Salahub, O. L. Malkina, and V. G. Malkin, J. Chem. Phys. **110**, 7153 (1999).
[37] R. E. Wasylishen, J. O. Friedrich, S. Mooibrock, and J. B. Macdonald, J. Chem. Phys. **83**, 548 (1985).
[38] C. H. Townes and A. L. Schawlow, *Microwave Spectroscopy* (Ref. [34]), p. 279.
[39] J. Vanier and C. Audoin, *The Quantum Physics of Atomic Frequency Standards* (Ref. [35]), p. 797.
[40] A. Clairon, P. Laurent, G. Santarelli, S. Ghezali, S. N. Lea, and M. Bahoura, IEEE Trans. Instrum. Meas. **44**, 128 (1995).
[41] A. D. Ludlow, M. M. Boyd, T. Zelevinsky, S. M. Foreman, S. Blatt, M. Notcutt, T. Ido, and J. Ye, Phys. Rev. Lett. **96**, 033003 (2006).
[42] J. F. Mijangos, J. M. Brown, F. Matsushima, H. Odashima, K. Takagi, L. R. Zink, and K. M. Evenson, J. Mol. Spectrosc. **225**, 189 (2004).